Tellus (2000), 52B, 452–462
Printed in UK. All rights reserved

TELLUS
ISSN 0280–6509

Evolution of boundary-layer aerosol particles due to in-cloud chemical reactions during the 2nd Lagrangian experiment of ACE-2

By ANTHONY J. DORE[1]*, DOUGLAS W. JOHNSON[2], SIMON R. OSBORNE[2], THOMAS W. CHOULARTON[4], KEITH N. BOWER[1], MEINRAT O. ANDREAE[3] and BRIAN J. BANDY[4], [1]*Physics Department, UMIST, Manchester, UK;* [2]*Meteorological Research Flight, DERA, Farnborough, UK;* [3]*Biogeochemistry Department, Max Planck Institute for Chemistry, Mainz, Germany;* [4]*School of Environmental Sciences, University of East Anglia, Norwich, UK*

(Manuscript received 8 February 1999; in final form 20 September 1999)

ABSTRACT

The second Aerosol Characterisation Experiment (ACE-2) was aimed at investigating the physical, chemical and radiative properties of aerosol and their evolution in the North Atlantic region. In the 2nd "Lagrangian" experiment, an air mass was tracked over a 30-h period during conditions of extensive stratocumulus cover. Boundary-layer measurements of the aerosol size distribution obtained with a passive cavity aerosol spectrometer probe (PCASP) during the experiment show a gradual growth in size of particles in the 0.1–0.2 μm diameter mode. Simultaneously, SO_2 concentrations were found to decrease sharply from 800 to 20 ppt. The fraction of sulphate in aerosol ionic mass increased from 0.68 ± 0.07 to 0.82 ± 0.09 for small particles (diameter below 1.7 μm) and from 0.21 ± 0.04 to 0.34 ± 0.03 for large particles (diameter above 1.7 μm). The measurements were compared with a multicyclic parcel model of gas phase diffusion into cloud droplets and aqueous phase chemical reactions. The model was able to broadly reproduce the observed transformation in the aerosol spectra and the timescale for the transformation of SO_2 to sulphate aerosol. The modelled SO_2 concentration in the boundary layer fell to below half its initial value over a 6.5-h time period due to a combination of the entrainment of cleaner tropospheric air and cloud chemical reactions. NH_3 and HCl gas were also found to play an important rôle in cloud processing in the model.

1. Introduction

Aerosol particles are known to play an important and complex rôle in determining cloud properties. The size, number concentration and solubility of aerosol particles present influence the number concentration and size distribution of cloud droplets formed for a given supersaturation. Changes in aerosol numbers and chemistry therefore affect the number of cloud condensation nuclei (CCN) entering cloud base. For a given liquid water content this implies a change in cloud droplet number concentration, affecting the radiative properties and precipitation tendencies of the cloud. More recently however, it has become evident that the interaction between clouds and aerosol is a more complex 2-way process. The aqueous phase is the state in which much of the atmosphere's chemical processes take place. In particular, part of the sulphur cycle involves the diffusion of SO_2 gas into cloud droplets and

* Corresponding author: Anthony Dore, Physics Department, UMIST, PO Box 88, Manchester M60 1QD, UK.
e-mail: anthony.dore@umist.ac.uk

subsequent oxidation by O_3 and H_2O_2. This, as well as other aqueous phase reactions, can cause a significant increase in the concentration of ions dissolved in cloud water, particularly if the cloud is long lived and in the presence of excess gaseous concentrations. Cloud droplets which have been subjected to such chemical reactions can be transported by turbulent motion to cloud edge where evaporation leads to the formation of aerosol particles with increased mass. This is particularly significant amongst smaller particles which undergo a greater mass change in proportion to their original mass.

Ground based experiments have been conducted using a hill cap cloud to investigate the transformation in aerosol properties resulting from cloud processing. Bradbury et al. (1999) noted a loss of aerosol particles in the range 0.05 to 0.13 μm diameter after passage through the Great Dun Fell cap cloud. Results from aircraft experiments have also shown the effect of cloud processing on aerosol size distribution. The Monterey Area Ship Track (MAST) experiment involved the use of instrumented aircraft to investigate the interaction of anthropogenic aerosol and stratocumulus cloud. It was found that a dip in the aerosol spectrum at 0.1 μm diameter could form within a timescale of a few hours (Durkee et al., 1998). Hoppel et al. (1994) made measurements of the aerosol size distribution and gas concentrations from an airship operating off the coast of Oregon. The processing of aerosol through stratus cloud was found to cause an increase in mass of the CCN with a distinct cloud residue mode in the the aerosol size distribution detected below cloud base. The climatological impact of multiple processing of aerosol particles in stratocumulus clouds has been assessed by Bower et al. (1999). The 1st cloud cycle modelled was found to introduce the most modification to the aerosol size distribution with further modification being limited by hydrogen peroxide concentrations. The modification of the aerosol population was found to have little effect on the microphysics of the processing cloud but gave processed aerosols the potential to act as more efficient cloud condensation nuclei in less vigorous clouds. In additional to aqueous phase reactions, the effects of collision-coalesence of cloud droplets can also serve to modify boundary-layer aerosol properties. Numerical simulations made by Feingold et al. (1996) showed that this process could produce a similar increase in mean particle size to that caused by chemical reactions. For remote maritime conditions, aqueous phase chemistry was more important at low liquid water contents whereas collision-coalesence dominated at higher liquid water contents. A box model was used by Raes (1995) to study the formation of new particles from di-methyl sulphide (DMS) in the marine boundary layer (MBL) and exchange of particles between the free troposphere and the cloudy marine boundary layer. The results suggest that variations in the number concentration of aerosols in the marine boundary layer are determined by properties of the free troposphere aerosol whereas variations in the sulphate mass of boundary-layer aerosol depend on the DMS flux. Fitzgerald et al. (1998) used a one-dimensional, multicomponent sectional model to simulate the temporal and vertical variations of the aerosol size distribution and composition in the MBL. The simulations showed that the effect of cloud processing in the upper part of the MBL is manifested at the surface on a timescale that is much faster than changes due to exchange with the free troposphere. However it was found that the free troposphere could be a significant source of particles for the MBL in the size range between the unactivated interstitial particles and the cloud condensation nuclei.

Here we present the results of a Lagrangian experiment when a polluted air mass was advected in a south westerly direction from the Iberian peninsula across the Atlantic ocean. Measurements made during a 30-h time period during conditions of persistent stratocumulus allow us to investigate the influence of cloud processing on aerosol evolution in the marine boundary layer. The results are compared to a parcel model of cloud chemical reactions which incorporates the take up into solution of SO_2, NH_3 and HCl gas. Aqueous phase reactions include the oxidation of sulphur(IV) by O_3 and H_2O_2 and also by O_2, catalysed by Fe and Mn.

2. Field experiment

The "Lagrangian" experiment was one of several separate experiments comprising the ACE-2 project (Raes et al., 2000). During this experiment a

parcel of air was tagged with constant level balloons and poly-fluoro-carbon tracer gas. The UK Meteorological Office C-130 Hercules aircraft was used to monitor the evolving aerosol and cloud properties in the tagged air parcel over time periods of 30 to 40 h. Three full Lagrangian experiments were conducted, each comprising 3 individual flights. An overview of the Lagrangian experiment is presented in Johnson et al. (2000). The 2nd Lagrangian experiment occurred in a polluted air mass which passed over southwest Europe before moving south towards Tenerife where the ACE-2 experiment was based. Measurements were made from 2000 UTC on 16 July till 0400 UTC on 18 July 1997 during the presence of wide-spread stratocumulus cloud cover. A more detailed analysis of the evolution of the boundary layer during this case study is presented by Osborne et al. (2000). The flight patterns for this experiment (illustrated in Johnson et al., 2000) consist primarily of box patterns at different altitudes that drift with the tagged air parcel. The side of each box represents a 7-min run, corresponding to a distance of approximately 42 km. Aditionally, a number of profiles were made through the boundary layer and troposphere. A comparison of the flight tracks of the aircraft with balloon trajectories shows that the aircraft was successful in sampling the same parcel of air throughout the experiment.

Fig. 1 shows the altitude of cloud base and cloud top, as measured by the forward scattering spectrometer probe (FSSP), as a function of time during the 3 flights. The stratocumulus layer increases in height between the 1st and 2nd flights. During the 2nd flight, a detached layer of broken cumulus cloud was present below the stratocumulus. By the time of the 3rd flight the cumuli were fewer in number and the cloudy layer was deeper. A single measurement of cloud top or cloud base height can be obtained to an accuracy of approximately ± 20 m with the FSSP. Variability in these values however arises due to the natural inhomogeneity of cloud in the measurement area. The depth of the boundary layer was found to increase from 490 ± 100 m at the start of the experiment to 1050 ± 50 m at the end.

Analysis of turbulence data recorded by the aircraft reveals stronger updraughts in cloud during successive flights. Root mean square vertical wind speeds were calculated from the raw data logged at 32 Hz. The values from level in-cloud runs were found to increase from 0.34 m s^{-1} during the 1st flight to 0.48 m s^{-1} during the 2nd flight and 0.55 m s^{-1} for the 3rd.

Two instruments were used to count the number concentration of aerosol particles. These were the passive cavity aerosol spectrometer probe (PCASP) which counts particles in the size range 0.1 to 3.0 μm diameter and the Condensation Nuclei (CN) detector which counts particles with diameter >3 nm. Fig. 2 shows the transformation in the dehydrated accumulation mode of the aerosol spectrum measured by the PCASP during the 3 flights with error bars derived from the standard deviation of the numbers logged during the sampling period. The growth in size of the small particles during the measurement period is thought to be due to cloud processing where the smallest particles activated at cloud base are those

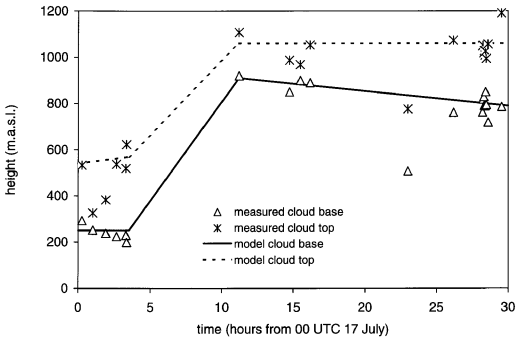

Fig. 1. Development of the cloudy layer as measured by the FSSP on the C-130 and the representation of the cloud layer in the model.

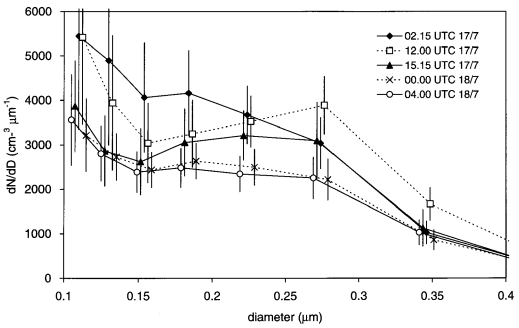

Fig. 2. Evolution of the measured dehydrated aerosol size distribution measured with the PCASP in the boundary layer from 30-min averages.

with radius about 0.15 μm diameter. Chemical reactions in cloud result in a significant increase in the size of these small particles, modifying the aerosol spectra. A general decrease in the number concentration of particles with time is also evident. This is probably caused by the diluting effect of entraining cleaner tropospheric air into the boundary layer.

The chemical composition of the inorganic fraction of the aerosol was determined by the collection on filters of hydrated particles segregated into size categories above and below 1.7 μm diameter (Andreae et al., 2000). Precautions were taken to avoid sample contamination with NH_3 and SO_2 from ambient air during sample collection and processing. Filters were handled in the lab in a clean-air bench fitted with scrubbers to remove NH_3 and SO_2. The filters were prepared and placed into the filter holders no more than 1 day before sampling and the complete filter assemblies were stored in gas-tight plastic housings. The Teflon filters, on which the ammonium ion is found, were in the middle of a 3-filter stack and thus protected on both sides by another filter. The filter samples were analysed by ion chromatography after dissolving the collected particulate matter in deionized water. Measurement error was taken to be the greater of: either the analytical error of the ion chromatographical measurements (4–10% depending on species) or: twice the standard deviation of the blanks. Using the known volume of air sample corresponding to each filter, the aerosol loadings of different chemical species can be determined. In the fine aerosol size fraction, the boundary-layer aerosol composition was initially dominated by NH_4^+ and SO_4^{--}. However the ratio of the concentrations of these 2 ions suggests that the particles were not composed entirely of $(NH_4)_2SO_4$ but also included some H_2SO_4. Aerosol loadings of all ions were found to decrease steadily, probably due to entrainment of cleaner air as illustrated in Fig. 3. By 0400 UTC the following day, the aerosol loadings of all ions had decreased to the following fractions of their original loadings: 0.77, 0.56, 0.21, 0.16, 0.30 and 0.10 for SO_4^{--}, NH_4^-, NO_3^-, Cl^-, Mg^{++} and Ca^{++} respectively. Although the ionic mass fraction of aerosol was initially dominated by sulphate (0.68 ± 0.07), the sulphate fraction increased further with time to 0.82 (± 0.09). In the lower troposphere, aerosol chemical loadings were generally significantly lower than in the boundary layer though stratified polluted layers were detected, notably at 0240 UTC when concentrations of NH_4^+ and SO_4^{--} similar to those in the boundary layer were measured. In the tropospheric sample, the ratio of NH_4^- to SO_4^{--} was 2.2 for the fine aerosol fraction so that the aerosol does not appear to have included the H^+ ion as was the case with the boundary-layer aerosol sample.

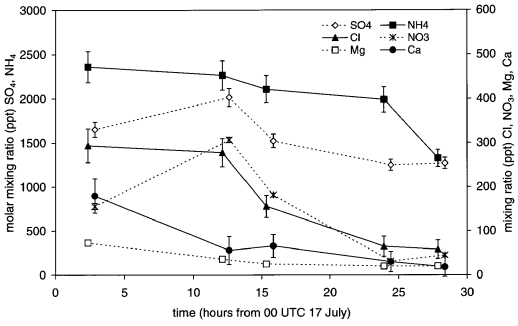

Fig. 3. Measured evolution of aerosol chemical composition in the boundary layer from filter collections (for sizes with diameter < 1.7 μm).

The large aerosol size category (diameter above 1.7 μm) was initially dominated by sea salt with mixing ratios of 1500 (± 100) ppt and 900 (± 60) ppt for boundary layer Na^+ and Cl^- at 0220 UTC. By 0350 UTC on 18 July, these concentrations had fallen to 0.51 and 0.37 of their initial values. This was caused principally by entrainment of cleaner tropospheric air though the greater loss of Cl^- may have been due to outgassing of HCl from the aqueous phase. The ionic mass fraction of SO_4^{--} in large boundary-layer aerosol was 0.21 (± 0.04) at the start of the experiment, below those for Na^+ and Cl^- (both 0.29 ± 0.05). At the end of the experiment however, the SO_4^{--} ionic mass fraction had grown to 0.34 (± 0.03). The difference in the chemical components of boundary layer and lower tropospheric air may in part be due to their different trajectories (illustrated in Johnson et al. (2000)). Back trajectory analysis from altitudes above 500 m (at the start of the experiment) shows that this air mass spent much of the previous 48 h passing over southern France and Iberia where it was in contact with sources of NH_3. However, back trajectories from below 500 m altitude pass mostly over the

ocean but touch the NW tip of Spain approximately 12 h prior to the start of the experiment, where SO_2 sources are present. In general, analysis of the chemical composition of boundary-layer aerosol shows that, as time progressed, sulphate became an increasingly important component. Total number concentrations of particles measured by the PCASP and CN counter in the boundary layer are shown in Fig. 4. The measurement error bars represent the standard deviation of the sampled data set. The total number of aerosol particles as measured by the CN counter declines sharply from 3400 cm^{-3} at the start of the experiment to below half this value by the end (1600 cm^{-3}). During one sample, taken from 11.48 UTC to 11.55Z UTC a large error bar occurs when the aircraft encountered a ship plume and the number concentration jumped for a period of about 10 s from around 3000 cm^{-3} to 20 000 cm^{-3}. This contamination source appears not to have strongly influenced the mean value calculated from this run. In general, the halving of aerosol numbers over a 24-h period due to dilution from entrainment is apparent.

Fig. 5 shows the observed trend in SO_2 concentrations. Measurement error was taken to be the greater of either the analytical error (6%) or twice the standard deviation of the blanks (Andreae et al., 2000). Boundary layer concentrations show a strong and steady decline from 800 ($\pm$60) ppt at 0200 UTC on 17 July to 14 ($\pm$11) ppt at 0000 UTC on 18 July. SO_2 concentrations measured in the lower troposphere just above cloud were generally lower, all samples being below 40 ppt, with the exception of one anomalously high sample of 760 ($\pm$60) ppt recorded at 0300 UTC in a polluted layer. This corresponds with high aerosol loadings also measured at this time as noted above. The consumption of SO_2 by aqueous phase chemistry and dilution by entrainment of cleaner tropospheric air are thought to be the primary processes for the decline in boundary layer concentrations. An additional process which has been proposed by O'Dowd et al. (1997) is the deposition of SO_2 onto sea-salt particles, thereby increasing the sea-salt sulphate.

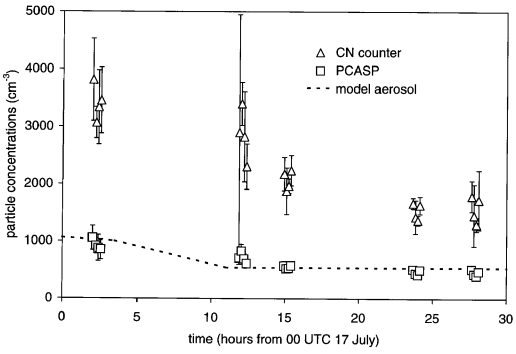

Fig. 4. Evolution of boundary layer aerosol number concentrations as measured by the C-130 (with the CN counter and the passive cavity aerosol spectrometer probe) and represented in the model.

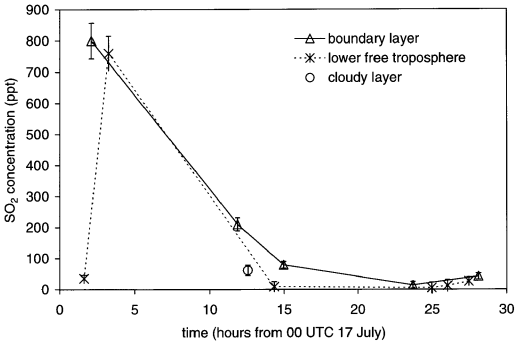

Fig. 5. Evolution of SO_2 concentrations as measured by filters on the C-130.

The total aerosol mass loading measured by the filters at the start of the experiment was 13.8 ($\pm$1.0) $\mu g\ m^{-3}$ and had decreased to 9.0 ($\pm$0.5) $\mu g\ m^{-3}$ by the end of the experiment. The influence of entrainment was observed to result in an increase in the depth of the boundary layer by a factor of 2.1 ($\pm$0.4). In the absence of any sinks or sources of aerosols and, assuming the entrained air was clean, the aerosol mass loading would have been reduced to 6.6 ($\pm$1.4) $\mu g\ m^{-3}$ at the end of the experiment. The difference between this and the measured value at the end of the experiment is 2.4 ($\pm$1.5) $\mu g\ m^{-3}$. This represents the net contribution to aerosol mass via conversion from the gas phase and from entrainment from the free troposphere but due to uncertainties in measurement of cloud properties and chemical analysis cannot be established accurately.

At the start of the experiment the total sulphur loading was 2.7 ($\pm$0.2) ppb, comprising 0.8 ($\pm$0.06) ppb of SO_2 and 1.9 ($\pm$0.1) ppb of sulphate aerosol. This had fallen to 1.6 ($\pm$0.1) ppb of sulphate

aerosol by the end of the experiment with only 0.04 ($\pm$0.01) ppb of SO_2. The diluting effect of the entrainment of clean air alone would be expected to halve the initial sulphur loading to 1.3 ($\pm$0.3) ppb. The implied net input required for the boundary layer sulphur mass balance to be conserved (0.3 ppb) is therefore not statistically significant as the error in estimation is the same as the value itself. Possible additional sources of sulphur include entrainment from the free troposphere and sea surface emissions.

An overall picture emerges from analysis of the chemical composition and number concentration of aerosol particles as well as gas phase data. A transformation of sulphur is occurring from the gas phase to the solid phase. Most probably this happens via in-cloud aqueous phase oxidation reactions. Entrainment from the troposphere provides a plentiful supply of oxidising gases to drive this process. Simultaneously the entrainment process has a strong diluting effect on the aerosol number concentration in the boundary layer.

3. Modelling studies

A parcel model of aqueous phase chemical reactions (Bower et al., 1991; Colvile et al., 1994; Sander et al., 1995; Bower et al., 1997; Flynn et al., 2000), previously used in orographic cap cloud simulations, was developed to model the multicyclic transformation of aerosols in layer clouds. Each aerosol size category incorporates a specified internal mixture of the following ionic species: Na^+, Cl^-, SO_4^{--}, NH_4^+, NO_3^-, H^+, OH^- and Fe^{+++} as well as an insoluble component. The aerosol is deliquesed in equilibrium with ambient air. Individual aerosol size categories are activated according to calculations of the critical radius from the Köhler equation (Sander et al., 1995). The number of cloud droplets formed therefore depends on the supersaturation which is determined by the prescribed updraught at cloud base. Once formed, cloud droplets continue to grow in size as the parcel moves upwards in the cloud according to the kinetic equation, incorporating droplet radius-dependent values for the diffusivity of water vapour and the thermal conductivity of air due to gas kinetic effects. Once the threshold volume mixing ratio of cloud liquid water (0.01 g m^{-3}) has been exceeded, aqueous phase chemistry occurs in droplets with radius >0.5 μm. The aqueous phase reactions include the oxidation of sulphur(IV) by O_3 and H_2O_2 and also by O_2, catalysed by Fe and Mn as well as oxidation by nitrate and chlorine radicals. Oxidation of NO to NO_3^- occurs via gas phase and aqueous phase pathways. The model is effectively a night-time model as no photochemical reactions are included. The diffusion of molecules from the gas phase in to solution (and vice-versa) is represented using the Henry constant to calculate the equilibrium gas phase constant and incorporating the effects of both gas phase diffusion and mass transport in the transfer coefficient. In non-cloudy air a gas phase chemical scheme is applied. This includes the oxidation of NO to NO_2 and subsequently to N_2O_5 which is converted to nitric acid in solution. The molecules CO_2, HCOOH, CH_3COOH, NH_3, HNO_2, HNO_3 and SO_2 are also present and although they are considered to be inert in the gas phase, they are soluble and can influence the acidity of the cloud dropets. A more detailed description of the chemical schemes included in the model is given in Sander et al. (1995).

The model was initialised with the size distribution of aerosol particles measured with the PCASP at 0215 UTC on 17 July (Fig. 2). The measured dehydrated aerosol sizes were converted to mass assuming an aerosol mass density of 2 g cm^{-3}. The input chemical loadings for each aerosol size category were then calculated using aerosol chemical composition from the filter measurements for the two size categories, above and below 1.7 μm diameter, discussed above. Particles with diameter <0.5 μm were assumed to be composed of NH_4^+ and SO_4^{--} in the measured ratio of 1.4 : 1 with the ion balance made up by H^+. The initial concentration of SO_2 was set at 800 ppt. Due to the significant input of oxidants from the free troposphere to the boundary layer in this case study, concentrations of H_2O_2 and O_3 were read from a temporal file generated from measurements (as in Fig. 6) at the start of each cloud cycle. Other gas concentrations, which may also play an important rôle in cloud processing, were not measured by the aircraft. Their input values were estimated based on measurements made at a coastal site at Tenerife on 18 July during the hill cloud experiment when the air was blowing from the sea. The following concentrations were used in the model: 500 ppt NH_3, 80 ppt NO_2, 500 ppt HCl and 5 ppt HNO_3.

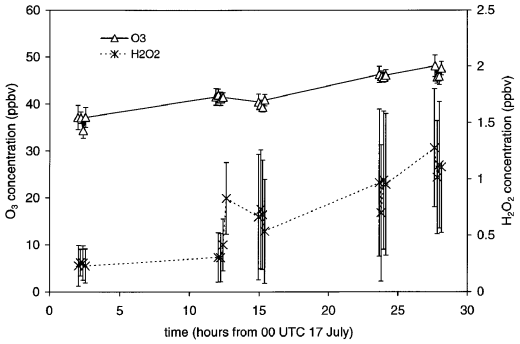

Fig. 6. Evolution of boundary layer H_2O_2 and O_3 concentrations measured by the C-130.

Cloud base and cloud top altitude were input at each cloud cycle from a temporal file as shown in Fig. 1. Cloud base started at 250 m at 0000 UTC on 17 July, growing to 910 m by 1100 UTC and finishing at 790 m at 0400 UTC on 18 July. Similarly cloud top started at 540 m, growing to 1060 m by 1100 UTC and finishing at 1060 m. Significant entrainment was clearly present during this experiment. Measurements of aerosol and SO_2 concentrations were made in the free troposphere (both profiles and constant altitude box patterns), discussed in Osborne et al. (1999). In general they showed much lower concentrations than in the boundary layer. It was therefore assumed in the model that the growth in depth of the boundary layer (cloud top) was representative of the amount of entrained air, which was clean and contained no aerosol or reactive gases. In practice then, a gradual dilution of aerosol numbers and gas concentrations occurred in the model, with the exception of H_2O_2 and O_3 which were restrained to increase in concentration, following the C-130 measurements, as discussed above. This simple representation of the entrainment process may be inappropriate however near the beginning of the simulation at approximately 0330 UTC when a polluted layer was detected above cloud. This layer appears to have been strongly stratified and it probably played a rôle in entraining polluted air in to the boundary layer, discussed in Osborne et al. (1999). However, due to the small number of measurements within this polluted layer, it is difficult to assess quantitatively its influence on the properties of the entrained air. For the purposes of the model therefore, the polluted tropospheric layer has been ignored.

The model takes a parcel of air and moves it up from the surface into cloud. After reaching cloud top, the parcel is moved back down to the surface. This represents one complete cloud cycle in the model. The number of cloud cycles performed by an air parcel during a given time therefore depends on the prescribed updraughts and the depth of the boundary layer. Such parcel updraughts are a somewhat non-physical feature of the model. In reality a parcel of aerosol particles in the boundary layer would be subject to variable vertical turbulent motion on different scales. An analysis of the boundary layer vertical windspeeds logged at 32 Hz by the aircraft showed that the r.m.s. vertical velocity was approximately 0.34 ($\pm$0.1) m s^{-1} at the start of the experiment, increasing to 0.55 ($\pm$0.15) m s^{-1} by the end. These values were used for the updraught in cloud to initialise the condensation of cloud droplets. A seperate vertical velocity was used for cycling the air parcel through the boundary layer. A smoothing process was applied to the raw windspeed data to filter out high frequency turbulence. The resulting signal revealed cells with dimensions on a scale of 5–10 km. The r.m.s. of this signal was typically of the order 0.05 to 0.12 m s^{-1}. A value of 0.08 m s^{-1} was therefore used to represent the parcel updraughts and downdraughts in non-cloudy air.

Fig. 7a shows the evolution of the modelled aerosol spectra. The lowest particle size category nucleation scavenged is 0.12 μm. A dip appears in the spectrum at about 0.18 μm due to the diffusion of gases into cloud droplets and aqueous phase oxidation. A general increase in particle mass across the spectrum is evident. However, the less massive particles, with diameter 0.15 to 0.2 μm, undergo a greater increase in relative mass and thus a greater increase in particle diameter. In the model, this leads to a broadening of the particle size category bin widths, or in physical terms a depletion of aerosol numbers in this size range. At the lower end of the particle size spectra, smaller cloud droplets are formed which are highly concentrated in sulphate and ammonium ions, particularly near cloud base. Due to Henry's law equilibrium between aqueous and gas phase concentrations, outgassing can occur in these circumstances, resulting in a loss of mass. This produces

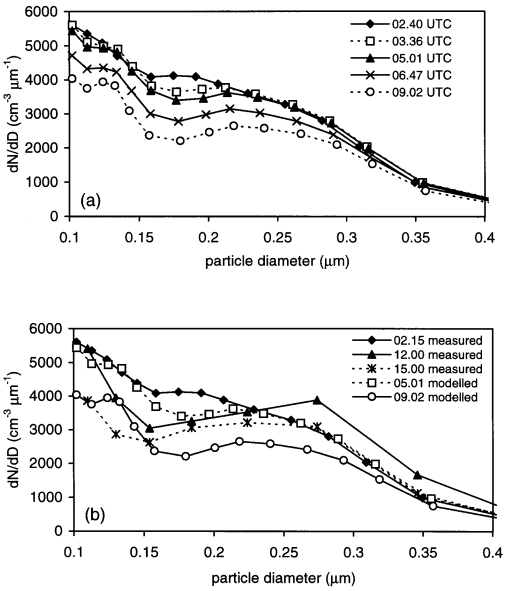

Fig. 7. (a) Modelled evolution of the aerosol size distribution during 4 cloud cycles, (b) inter-comparison of the measured and modelled aerosol size distributions.

a small peak in the spectrum at 0.12 µm diameter. Sensitivity studies with the model show that the outgassing can be much more significant when the fine aerosol is composed entirely of NH_4^+ and SO_4^{--} and the H^+ ion is not present. Although this outgassing effect has been observed in some experimental studies, it is not apparent from the aircraft measurements, as illustrated in Fig. 7b, where a comparison between the measured and modelled spectra is presented. A finer resolution of the size bins at the lower end of the PCASP spectrum would be necessary to investigate the process in detail. The dip which appears in the modelled spectrum at 0.18 µm occurs at a diameter slightly larger than that in the measured spectra (0.15 µm). Furthermore, the modelled dilution of aerosol numbers caused by the entrainment of clean air has resulted in a greater depletion of aerosol numbers in the size range 0.15–0.3 µm than was observed from the aircraft measurements.

The 4 cloud cycles in the model corresponds to a simulation time of approximately 6.4 h, ending at 0900 UTC. At this point the boundary layer height has increased to 900 m resulting in a significant decrease of total particle number concentration in the model. Generally the influence of cloud processing on the aerosol spectra is strongest during the 1st cloud cycle. By the 3rd cycle, gas concentrations have been significantly depleted by diffusion into the aqueous phase and the aerosol-gas mixture is tending towards a state of equilibrium. Further transformation of the spectra is mostly due to dilution by entrainment. Total aerosol numbers used in the model are shown in Fig. 4. It is interesting to note that the crude assumption, that clean air is entrained as the boundary layer grows, used in the model, provides a good agreement with the aerosol numbers measured by the PCASP. In reality though, this balance depends on other production and loss mechanisms. The former include sea salt production (wind dependent) and entrainment of polluted air from the free troposphere (which may have occurred at around 0300 UTC but is difficult to quantify due to the stratified nature of the polluted layer in the free troposphere). Loss mechanisms incude turbulent deposition of aerosol to the ocean surface and cloud collision coalesence (this is thought to be a significant process and will be the subject of future studies).

The evolution of the chemical loadings of aerosol are shown in Fig. 8a for particles in the size range 0.1–0.5 µm diameter and in Fig. 8b for

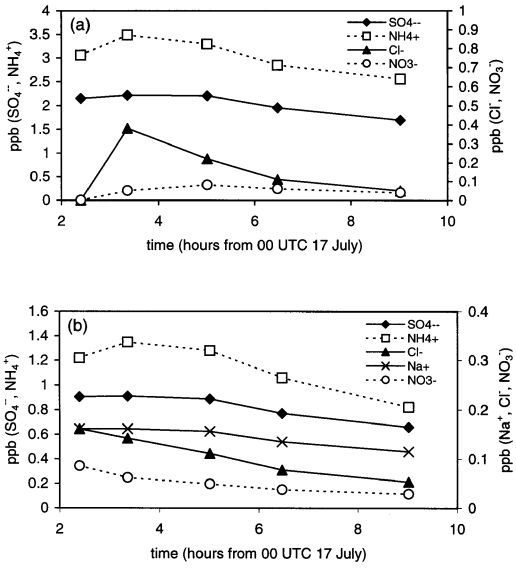

Fig. 8. Modelled evolution of aerosol chemical loadings: (a) for particles with diameter <0.5 µm, (b) for particles with diameter between 0.5 µm and 1.7 µm.

particles in the size range 0.5–1.7 μm diameter. The fine aerosol size fraction is initially composed of acid ammonium sulphate. During the 1st cycle, the increases in the loading of Cl^- and NH_4^+ are most notable, although much of the Cl^- acquired during the 1st cycle is lost by outgassing during further cloud cycles. A small increase in the SO_4^{--} loading occurs during the 1st cycle after which ion loadings generally show a decrease due to entrainment. A similar trend is evident with the ion loadings in the 0.5 to 1.7 μm size fraction. These particles however initially consisted of an internal mixture which included small amounts of Na^+, Cl^- and NO_3^-. The Na^+ ion is a non-reactive substance in the model so that the divergence of Cl^- and Na^+ ions is representative of outgassing of HCl.

Fig. 9 shows the modelled temporal trend in gas concentrations at the beginning of the simulation and after successive cloud cycles. The SO_2 concentration shows a steady decline over the 4 cloud cycles and by 0900 UTC has fallen from 0.8 ppb to 0.33 ppb. This represents a good agreement with the measured boundary layer SO_2 concentration which showed a similar decrease in concentration over the same time period. NH_3 is taken up rapidly by cloud droplets in the 1st cycle, declining in concentration from 0.5 ppb to 0.03 ppb and then gradually to 0.01 ppb. HCl is likewise consumed rapidly in the 1st cycle with concentrations falling from 0.5 ppb to 0.23 ppb and then gradually declining to 0.1 ppb. The NO_2 concentration, which is initially sustained by the slow gas phase conversion of NO, falls from 0.3 ppb to 0.15 ppb during the simulation. The baseline concentrations for these gases on the island of Tenerife on 18 July (corresponding to the end of the Lagrangian experiment) were measured as the following: 0.2 ($\pm$0.02) ppb NH_3, 0.2 ($\pm$0.1) ppb HCl, 0.1 ($\pm$0.05) ppb NO_2 and 0.02 ($\pm$0.005) ppb NO. The modelled values of NO_2, NO and HCl are therefore trending towards their measured values at the end of the experiment whilst the NH_3 concentration in the model falls rapidly below its measured value at the end of the experiment. In the model these gases play a significant rôle in cloud processing of aerosol. Unfortunately, as these gases were not measured during the Lagrangian project, it is not possible to check their importance for cloud processing during this experiment. It is of use however to test the sensitivity of the model to variability in the input gas concentrations. To this end 4 additional simulations were performed with identical input values except for independently modifying the input NH_3 concentration to 2.0 and 0.1 ppb and the HCl concentration also to 2.0 and 0.1 ppb. The results, illustrated in Fig. 10, show that varying the input concentrations of NH_3 and HCl does not greatly influence the shape of the processed aerosol spectra. However, increased gas concentrations do result in significantly enhanced cloud processing and a more pronounced dip in the aerosol spectra. This is particularly important for NH_3 which is readily taken into solution by cloud droplets. Uncertainty in the input gas con-

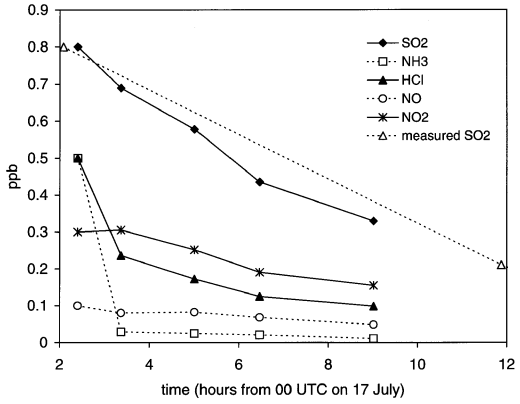

Fig. 9. Modelled evolution of gas concentrations during 4 successive cloud cycles with SO_2 concentration compared to the measurements.

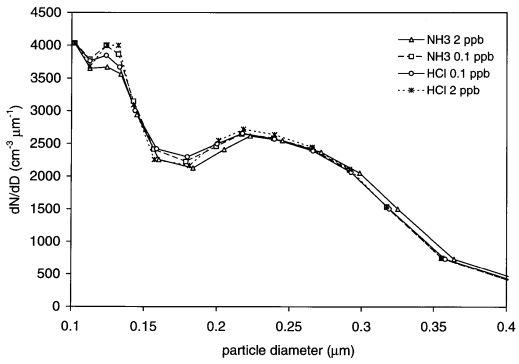

Fig. 10. Modelled evolution of the aerosol size distribution after 4 cloud cycles illustrating the influence of varying the input NH_3 and HCl gas concentrations.

centrations in the model can thus lead to an error of $\pm 5\%$ in the particle number concentration at the point of the dip in the aerosol spectrum.

Other sources of error include uncertainty in the updraught at cloud base. Sensitivity studies show that an uncertainty of $\pm 0.1\ \mathrm{m\ s^{-1}}$ in the updraught at cloud base corresponds to an uncertainty of $\pm 0.05\ \mu\mathrm{m}$ in the smallest particle size activated and thus in the location of the dip in the aerosol spectra. Furthermore the approach adopted in this model considers a parcel of air which is alternately entirely in cloud or entirely out of cloud. This may force cloud chemical processes to occur more rapidly than in a real turbulent cloudy boundary layer. An uncertainty of $\pm 0.02\ \mathrm{m\ s^{-1}}$ in the vertical speed of the parcel in the boundary layer was found to introduce an uncertainty of approximately 20% in the speed of cloud chemical processing. Fig. 11 illustrates the development of the modelled cloud liquid water content together with some gas phase concentrations during the 1st cloud cycle. Once droplet formation is initiated, the liquid water content grows adiabatically as the air parcel moves upwards, reaching a maximum of $0.75\ \mathrm{g\ m^{-3}}$ at cloud top. HCl gas is taken up rapidly by cloud droplets during the first few minutes of cloud formation though it is partially outgassed by the small droplets near cloud base when the air parcel cycles back down. A similar but less dramatic trend occurs with the H_2O_2 concentrations which reach a minimum near cloud top. In reality, the continued entrainment of fresh H_2O_2 from the lower free troposphere would drive the further aqueous phase oxidation of SO_2. In the model this is represented by refreshing the H_2O_2 concentrations at the start of each cloud cycle with the values measured during the experiment.

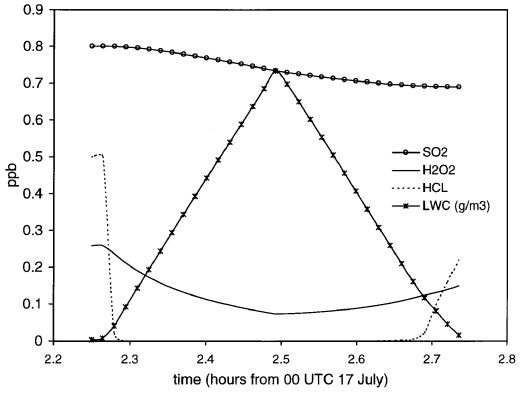

Fig. 11. The temporal trend of liquid water content and selected gas concentrations during the first modelled cloud cycle.

4. Conclusion

A Lagrangian experiment has been conducted over the North Atlantic using an instrumented aircraft to examine the evolution of aerosol properties in the marine boundary layer over a 29-h time period. The results show a transformation in the aerosol spectra with a dip appearing at about 0.15 μm. This was attributed to a growth in the size of small particles caused by aqueous phase oxidation of SO_2. Simultaneously a strong decrease in SO_2 concentrations and an increase in the ionic fraction of sulphate in the aerosol mass were observed. Total aerosol numbers decreased due to entrainment of cleaner air from the free troposphere.

A comparison has been made with the results of a parcel model incorporating aqueous phase chemical reactions. A dip in the modelled aerosol spectra evolved at a similar diameter to the observed spectra. SO_2 concentrations decreased from 0.8 ppb to 0.3 ppb over a 6.5-h time period due to a combination of dilution due to entrainment of clean air and aqueous phase oxidation causing a conversion to sulphate aerosol. Despite the simple parcel model used, the timescale for the sulphur transformation was in good agreement with the measurements. The model showed that HCl and HN_3 gas can also play a significant rôle in the processing of aerosols by cloud.

5. Acknowledgements

ACE-2 was funded by the Commission of European Communities (contract ENV-CT95-0032). Additional support was received for the Lagrangian experiment from the Department of the Environment, Transport and the Regions and for the modelling studies from the Natural Environment Research Council. MOA acknowledges support from the German Max Planck Society. Thanks are due to Mike Flynn for assistance with the model and to Gordon Inverarity for help with computing problems.

REFERENCES

Andreae, M. O., Elbert, W., Gabriel, R., Johnson, D. W., Osborne, S. and Wood, R. 2000. Soluble ion chemistry of the atmospheric aerosol and SO_2 concentrations over the eastern North Atlantic during ACE-2. *Tellus* **B**, this issue.

Bower, K. N., Hill, T. A., Coe, H. and Choularton, T. W. 1991. SO_2 oxidation in an entraining cloud model with explicit microphysics. *Atmos. Env.* **25A**, 2401–2418.

Bower, K.N., Choularton, T. W., Gallagher, M. W., Colvile, R. N., Wells, M., Beswick, K. M., Wiedensohler, A., Hansson, H. C., Svenningsson, B., Swietlicki, E., Wendisch, M., Berner, A., Kruisz, C., Laj, P., Facchini, M. C., Fuzzi, S., Bizjak, M., Dollard, G., Jones, B., Acker, K., Wieprecht, W., Preiss, M., Sutton, M. A., Hargreaves, K. H., StoretonWest, R. L., Cape, J. N. and Arends, B. G. 1997. Observations and modelling of the processing of aerosol by a hill cap cloud. *Atmos. Env.* **31**, 2527–2544.

Bower, K. N., Jones, A. and Choularton, T. W. 1999. A modelling study of aerosol procesing by stratocumulus clouds and its impact on GCM parameterisations of clouds and aerosols. *Atmos. Res.* **50**, 317–344.

Bradbury, C., Bower, K. N., Choularton, T. W., Swietlicki, E., Birmili, W., Wiedensohler, A., Yuskiewicz, B., Berner, A., Dusek, U., Dore, C. J. and Fayden, G. G. 1999. Modelling of aerosol modification resulting from passage through a hill cap cloud. *Atmos. Res.* **50**, 185–204.

Colvile, R. N., Sander, R., Choularton, T. W., Bower, K. N., Inglis, K. W. F., Wobrock, W., Schell, D., Svenningson, I. B., Wiedensohler, A., Hansson, H.-C., Hallberg, A., Ogren, J. A., Noone, K. J., Facchini, M. C., Fuzzi, S., Orsi, G., Arends, B. G., Winiwarter, W., Schneider, T. and Berner, A. 1994. Computer modelling of clouds at Kleiner Feldberg. *J. Atmos. Chem.* **19**, 189–229.

Durkee, P. A., Noone, K. J., Ferek, R. J., Johnson, D. W., Taylor, J. P., Garrett, T. J., Hobbs, P. V., Hudson, J. G., Brotherton, C. S., Innis, G., Frick, G. M., Hoppel, W. A., O'Dowd, C., Russell, L. M., Gasparovic, R., Nielsen, K. E., Ostrom, E., Osborne, S. R., Flagan, R. C., Seinfield, J. H. and Rand, R. 2000. The impact of ship-produced aerosols on the microphysical characteristics of warm stratocumulus clouds: a test of MAST hypotheses 1.1a and 1.1b. *J. Atmos. Sci.*, in press.

Feingold, G., Kreidenweis, S. M., Stevens, B. and Cotton, W. R. 1996. Numerical simulations of stratocumulus processing. *J. Geophys. Res.* **101**, D16, 21,391–21,402.

Fitzgerald, J.W., Marti, J. J., Hoppel, W. A., Frick, G. M. and Gelbard, F. 1998. A one-dimensional sectional model to simulate multicomponent aerosol dynamics in the marine boundary layer — 2. Model application. *J. Geophys. Res.* **103**, D13, 16,103–16,117.

Flynn, M., Bower, K. N., Choularton, T. W., Wobrock, W. and Mäkelä, J. M. 2000. Modelling cloud processing of aerosol during the ACE-2 Hillcloud experiment. *Tellus* **B**, this issue.

Hoppel, W. A., Frick, G. M. and Larson, R. E. 1994. Marine boundary-layer measurements of new particle formation and the effects non-precipitating clouds have on aerosol size distribution. *J. Geophys. Res.* **99**, D7, 14,443–14,459.

Johnson, D. W., Osborne, S. R., Wood, R., Suhre, K., Andreae, M. O., Johnson, R., Businger, S., Quinn, P. K., Bates, T., Durkee, P., Jonson, H., Russell, L. M., Noone, K., Glantz, P., Bandy, B., O'Dowd, C., Rapsomanikis, S. and Rudolph, J. 2000. An overview of the Lagrangian experiments undertaken during the north Atlantic regional aerosol characterisation experiment (ACE-2). *Tellus* **B**, this issue.

O'Dowd, C. D., Lowe, J. A., Smith, M. H., Davison, B., Hewitt, N. and Harrison, R. M., 1997. Biogenic emissions and inferred non-sea-salt sulphate cloud condensation nuclei in and around Antartica. *J. Geophys. Res.* **102**, D11, 12,839–12,854.

Osborne, S. R., Johnson, D. W., Wood, R., Bandy, B. J., Andreae, M. O., O'Dowd, C. D., Glantz, P. and Noone, K. 2000. Observations of the aerosol, cloud and boundary layer dynamic and thermodynamic characteristics during the 2nd Lagrangian experiment of ACE-2. *Tellus* **B**, this issue.

Raes, F. 1995. Entrainment of free tropospheric aerosols as a regulating mechanism for cloud condensation nuclei in the remote marine boundary-layer. *J. Geophys. Res.* **100**, D2, 2893–2903.

Raes, F., Bates, T. S., McGovern, F. M. and van Liedekerke, M. 2000. The second Aerosol Characterisation Experiment (ACE-2): general overview and main results. *Tellus* **B**, this issue.

Sander, R., Leliveld, J. and Crutzen, P. J. 1995. Modelling of the night time nitrogen and sulphur chemistry in size resolved droplets of an orographic cloud. *J. Atmos. Chem.* **20**, 89–116.